UDC 004.93
DOI: 10.15587/1729-4061.2022.265066

DEVISING A METHOD FOR PREDICTING A BLOOD PRESSURE LEVEL BASED ON ELECTROCARDIOGRAM AND PHOTOPLETHYSMOGRAM SIGNALS

Alexey Savostin
Candidate of Technical Sciences, Professor*
Amandyk Tuleshov
Doctor of Technical Sciences, Professor, CEO, Head of Laboratory
Laboratory of Intelligent Robotic Systems
U. Joldasbekov Institute of Mechanics and Engineering
Shevscenko str., 28, Almaty, Republic of Kazakhstan, 050010
Kayrat Koshekov
Doctor of Technical Sciences, Professor
Department of Science and International Cooperation
Academy Civil Aviation
Akhmetova str., 44, Almaty, Republic of Kazakhstan, 050039
Galina Savostina
Corresponding author
Doctor PhD, Associated Professor*
E-mail: gvshubina@ku.edu.kz
Alexandr Largin
Doctoral Student*
*Department of Energetic and Radioelectronics
Manash Kozybayev North Kazakhstan University
Pushkin str., 86, Petropavlovsk, Republic of Kazakhstan, 150000

Determining the level of blood pressure (BP) in a non-invasive way and without a sphygmomanometer cuff is of great relevance when conducting continuous monitoring or screening studies. In this regard, a method for predicting BP parameters based on the signals of the photoplethysmogram (PPG) and electrocardiogram (ECG) signals has been developed. It is proposed to use, as informative features, the time of pulse wave propagation (PTT) and a set of calculated pulse parameters of PPG. PTT is defined as the time intervals between the R-wave of the ECG and the corresponding characteristic points on the PPG acquired optically from the finger. As parameters of the PPG pulse, the known characteristics of this signal described in the literature are used, as well as additional informative features selected during the study.

In accordance with the above, the tools of machine learning theory were used to construct a classifier model and regression models. The approach described in this paper to determine BP makes it possible to use 10-second ECG signals in any of the 12 common leads and PPG signals from any optical type of sensor.

The built model of the classifier detects three levels of BP: low, normal, and high, at the accuracy metric=0.8494. The regression models predict systolic, diastolic, and mean BP parameters in accordance with the requirements of the British Hypertension Society (BHS) standard by the magnitude of the absolute error.

The proposed method for assessing the level of BP involves real-time measurements and can be used in the design of measuring equipment for screening studies, as well as in continuous monitoring tasks within the framework of BHS requirements

Keywords: blood pressure, machine learning, photoplethysmogram, bioelectric signals, pulse wave propagation time

Received date 20.07.2022
Accepted date 13.09.2022
Published date 30.10.2022

***How to Cite**: Savostin, A., Tuleshov, A., Koshekov, K., Savostina, G., Largin, A. (2022). Devising a method for predicting a blood pressure level based on electrocardiogram and photoplethysmogram signals. Eastern-European Journal of Enterprise Technologies, 5 (3 (119)), 62–74. doi: https://doi.org/10.15587/1729-4061.2022.265066*

1. Introduction

According to a 2021 study, worldwide, the number of people aged 30 to 79 years with hypertension doubled from 331 million women and 317 million men in 1990 to 626 million women and 652 million men in 2019 [1]. At the same time, according to estimates by the World Health Organization (WHO), 46 % of adults with hypertension are unaware of the presence of the disease [2]. Uncontrolled hypertension can be the cause of extremely dangerous complications, including angina pectoris, myocardial infarction, heart failure, arrhythmia, and stroke.

It is known [3] that hypertension is characterized by an excessive increase in blood (arterial) pressure, which, in turn, is a force acting on the arteries during blood circulation.

BP can be considered a periodic signal with a frequency equal to heart rate (HR). This signal is characterized by two main parameters: a maximum in the form of systolic pressure (SP) and a minimum – diastolic pressure (DP). SP occurs in the blood vessels at the time of contraction of the heart. DP emerges when the heart is at rest between two contractions.

The diagnosis of "hypertension" is assigned at SP≥140 mmHg and/or DP≥90 mmHg [3]. Although BP varies depending on the time of day, physical exertion, emotional state, food intake, and other factors, its regular measurement guarantees the identification of elevated indicators and, therefore, effective control and prevention of the development of hypertension.

For non-invasive determination of BP, sphygmomanometers are most widely used, providing high measurement accuracy. These devices consist of a manometer for measuring air pressure; a special cuff worn on the patient's arm, as well as an air blower equipped with an adjustable descent valve. The use of a sphygmomanometer causes certain inconvenience to the patient due to the use of a cuff that squeezes the arteries. In this regard, this technique is inconvenient for screening where maximum simplicity and speed of measurements are required.

In addition, sphygmomanometers cannot be used for long-term continuous monitoring of BP since constant compression of the cuff can affect the tone of the patient's vessels and skin. In widespread practice, long-term monitoring of BP is performed in an invasive way, when a catheter is placed in a blood vessel to gain direct access to the arterial bed [4]. It is obvious that this method is painful for the patient, has contraindications, requires specialized equipment and constant monitoring.

Due to these circumstances, researchers are currently paying great attention to the search for methods for measuring BP, devoid of these shortcomings. It is required to provide an acceptable level of measurement accuracy with minimal discomfort for the patient and the possibility of continuous monitoring. It should also be possible to apply the proposed method without taking into consideration the individual characteristics of the patient.

Thus, devising a method for non-invasive assessment of the level of BP of acceptable accuracy without the use of a sphygmomanometer cuff, and not requiring individual calibration, is timely and relevant.

2. Literature review and problem statement

The most promising in this area are indirect measurements based on the established relationship between the BP and pulse wave propagation rate, Pulse Wave Velocity (PWV) [5].

According to [5], the pulse wave is formed as a result of the movement of blood exerting pressure on the elastic walls of blood vessels and is perceived as a pulse. It is shown that the time in which a pulse wave travels a certain distance along the artery (Pulse Transit Time, PTT) is inversely proportional to PWV and can be used to determine BP.

It has been established that BPP and PTT can be related via the following dependence [6]:

$$P = C_1 \frac{1}{PTT} + C_2, \tag{1}$$

where C_1 and C_2 are some constants depending on the length of the artery section, the thickness of the vessel walls, the elasticity of the vessel walls, the density of the blood, as well as the diameter of the lumen of the vessel, and, consequently, varying over time and from person to person.

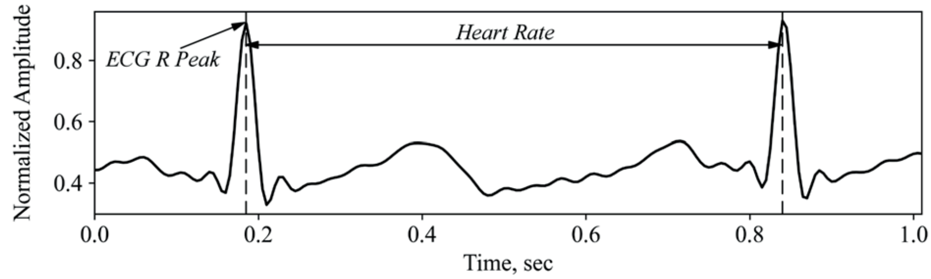

a

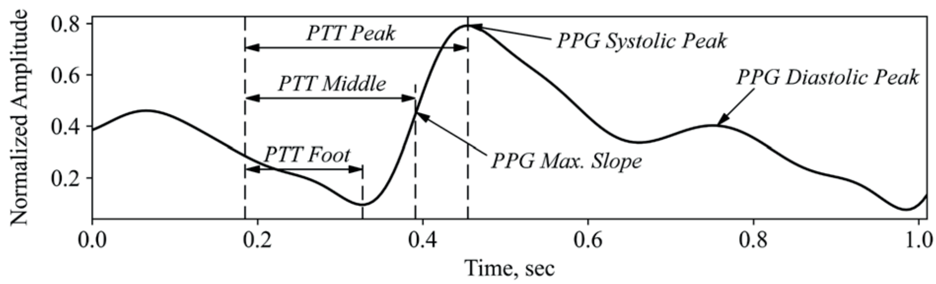

b

Fig. 1. Determining Pulse Transit Time using an electrocardiogram and a photoplethysmogram, recorded synchronously: *a* — electrocardiogram; *b* — photoplethysmogram

For (1), the PTT value can be estimated as the time interval between the *R* wave on the ECG and the corresponding point on PPG. Fig. 1, *a* shows the fragment of the ECG signal in the first standard lead, and Fig. 1, *b* – the PPG, recorded synchronously with the ECG optically from the finger.

As follows from Fig. 1, there are several options for determining *PTT*. PTT Peak is the time between the maximum of the R-wave of the ECG and the maximum of the PPG (systolic peak). PTT Foot is the time interval between the maximum of the R-wave of the ECG and the minimum of the PPG. PTT Middle is the time between the maximum of the R-wave of the ECG and the maximum of the first derivative of the PPG (Max. Slope).

It should be noted that in a number of studies it is proposed to use additional parameters related to the functioning of the cardiovascular system, for example, *hr* heart rate and previous measurements P_{n-1} to improve accuracy in determining the BP [7]:

$$P_n = C_1 \ln \mathrm{PTT} + C_2 \cdot hr + C_3 P_{n-1} + C_4. \tag{2}$$

For models (1) and (2), the values of C_i can be obtained by primary calibration, the procedure of which is described in the literature and tested in the laboratory [6, 8].

The need for calibration significantly narrows the scope of use of models such as (1) or (2) when assessing the level of BP. At the same time, devising a method that does not require calibration will allow it to be used for extensive screening studies, and will also greatly simplify the task of continuous monitoring.

To solve this problem, work [9] proposes to use, in addition to PPG data, personal characteristics of a person, such as gender, age, weight, body mass index, etc. It is obvious that such a solution is inconvenient for screening and is actually comparable to preliminary calibration.

In [10], the authors propose a promising method for determining PTT based on the measurement of bioimpedance. However, the study does not provide information on the results obtained on the prediction of BP.

In work [11], for training regression models, among others, signs are used that are automatically extracted from the ECG signal. At the same time, a database [12] is used to train models, in which compression algorithms were used for ECG signals, which greatly limits the possibility of automatic analysis. In such a situation, the solutions proposed in [11] are controversial.

In studies [13, 14], the size of the training sample is limited, which does not make it possible to unambiguously interpret the results obtained. In addition, to solve the described problem, the authors of [15] use the procedure of registration of PPG from two limbs (arm and leg) with a sampling frequency of 2500 Hz, which imposes significant restrictions on the type of sensor used and the simplicity of signal registration.

In study [16], in addition to the PPG data, heart rate variability (HRV) parameters are used as additional informative signs. This requires the analysis of long recordings of signals from 5 minutes and above. This approach greatly narrows the scope of application of the BP prediction method described in [16] both in screening tasks and in continuous monitoring.

Thus, our review of the literature data [10, 11, 13–16] shows the existence of an actual problem of measuring blood pressure by a non-invasive method without a sphygmomanometer cuff and without preliminary calibration. The solutions to this problem proposed in the literature have significant drawbacks such as a small size of the training sample, the extraction of informative signs of their ECG on the basis of [12], the need to personalize measurements, the lack of a methodology for measuring, the use of HRV features. Therefore, measurement methods should be improved for practical use. This confirms the need for new research aimed at developing a non-invasive method for predicting the level of BP from ECG and PPG signals.

3. The aim and objectives of the study

The purpose of this study is to devise a non-invasive method for predicting the level of BP according to the data of PPG and ECG signals. This will make it possible to design new measuring equipment, which, without prior individual calibration and with acceptable accuracy, will make it possible to solve the tasks of screening and monitoring the level of BP.

To accomplish the aim, the following tasks have been set:

– to define informative features from the studied signals and build a training data set;

– to find the optimal model of the classifier according to the known quality metrics;

– to determine the strategy for training the classifier model;

– to build regression models for predicting the value of systolic, diastolic, and mean BP, as well as to propose a general method of forecasting.

4. The study materials and methods

When building models, the study used a dataset from [17], compiled to construct algorithms for estimating BP without using a cuff. This database includes ECG signals for the second standard lead, PPG from the finger, and blood pressure (BP). This dataset was formed from records selected from The Multi-parameter Intelligent Monitoring in Intensive Care (MIMIC) II database [12].

All signals in this database have a sample rate of 125 Hz and a bit depth of at least 8 bits. As a result, the dataset used to build the models contains 12,000 records with a total duration of 741.53 hours from about 1,000 different patients. Fig. 2 shows a fragment of a synchronous recording of three signals from this dataset.

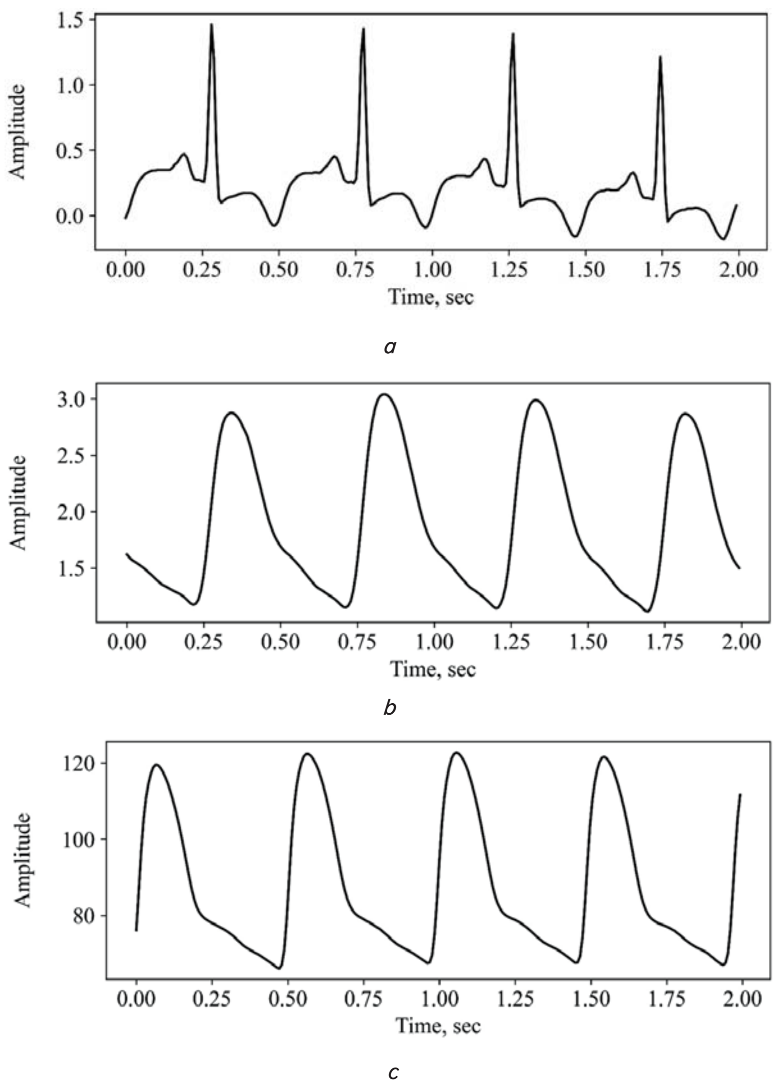

Fig. 2. Fragment of synchronous recording of three signals: *a* — electrocardiogram; *b* — photoplethysmogram; *c* — blood pressure

Information on BP indicators is determined by the signal of blood pressure: SP – the maximum signal on the analyzed time period; DP is its minimum in the section. The mean BP (MeanP) is calculated using the formula MeanP=1/3 (SP–DP)+DP [18]. To obtain more variable values of BP and take into consideration the dynamics of their change, the long records from the data set were divided into segments of 10 s duration (1250 samples), and the parameters of the BP were calculated for them. As a result, Fig. 3 shows the distribution of SD and DP values within the obtained space of X objects in the form of a set of ten-second records.

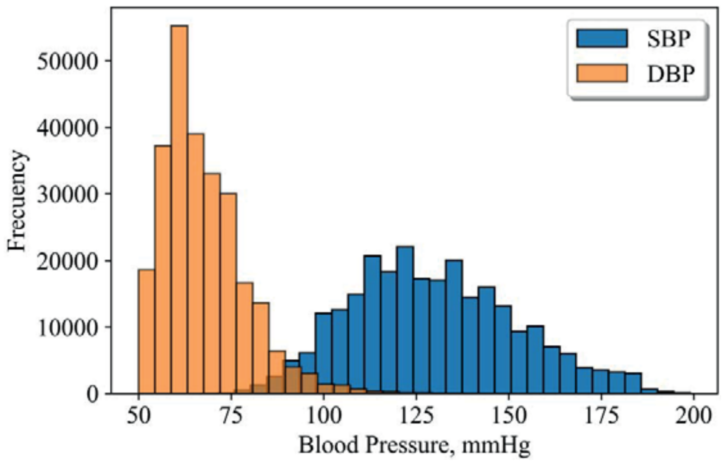

Fig. 3. Distribution of blood pressure indicators across the training data set

In accordance with the purpose of the study, we consider two approaches to building models for predicting BP: for screening studies, it is proposed to use a classifier model; for continuous monitoring tasks – regression models. These classes of models are developed using modern tools from the theory of machine learning (ML). The use of self-learning ML algorithms will reveal hidden patterns in the multidimensional space of the received informative features and summarize the results of forecasting for the general totality.

Based on the above, in order to solve the classification problem in accordance with [3, 19, 20], all records were divided into three classes according to the value of BP with the assignment of the label Y={0, 1, 2} as shown in Table 1.

Table 1

Division of samples according to BP level

Category	SP, mmHg	–	DP, mmHg	Class Y label
Low pressure	<90	or	<50	1
Normal pressure	90–129	and	50–84	0
High pressure	≥130	or	≥85	2

As a result, Table 2 gives the main statistical indicators of BP parameters for certain classes.

In Table 2, the following symbols are adopted: D – selective mean; sd – standard deviation; min is the minimum in a sample; max is the maximum in a sample. As follows from Table 2, the resulting number of samples in the classes is not balanced, which must be taken into consideration in the process of training the classifier model. It is also possible to note a higher variance of BP indicators for SP.

Prior to the extraction of informative features, the ECG and PPG signals were subjected to a high-frequency filtering procedure to remove low-frequency components in the range of 0–0.7 Hz. For this purpose, wavelet filtration was used, as a result of which the decomposition of ECG and PPG is performed to a level corresponding to low-frequency drift, zeroing of the obtained approximation coefficients, and subsequent restoration of signals. The Daubechies orthonormal wavelet (*db*8) is used as a wavelet function.

To train the classifier and regressor models, the values of PTT Peak (*ptt_p*), PTT Middle (*ptt_m*), and PTT Foot (*ptt_f*) were used, given in Fig. 1, *b*. In addition, for each ten-second interval, the heart rate (*hr*) was calculated.

In addition, it was decided to use additional informative features obtained on the basis of the characteristics of the pulse shape of the PPG signal since these parameters reflect the state of the cardiovascular system [21]. At the same time, informative features were not extracted from the available ECG signals since compression algorithms were used in the process of obtaining them, which do not make it possible to perform adequate automatic analysis [12].

Thus, in order to construct informative features, the parameters of the PPG pulses are calculated. To do this, first of all, it is necessary to determine the position of the characteristic points of the waveform.

The characteristic impulse points of the PPG, shown in Fig. 4, *a*, include the Minimum Point (Foot Point) F_i, the Systolic Peak S, the Diastolic Peak D, the Dicrotic Notch N, the Inflection Point I, and the Max. Slope point M.

In turn, to determine the position of these points, the first $P(t)$' and the second $P(t)$" derivatives of the PPG $P(t)$ signal are used according to the scheme shown in Fig. 4.

At the first stage of detecting characteristic points, the minima (point F_i in Fig. 4, *a*) and systolic maxima (point S) are searched. Since the shape of the PPG pulses is very variable, methods for determining the maxima in the signal that require setting the threshold or size of the search box may give low results. In this regard, in this work, for finding points F_i and S (Fig. 4, *a*) the algorithm of automatic multiscale-based peak detection (AMPD) in noisy periodic and quasi-periodic signals is used [22]. This algorithm does not use a fixed threshold procedure, and the size of the search box is scaled automatically.

Table 2

Statistical indicators of BP parameters by class

Class Y label	DP, mmHg				SP, mmHg				Number of samples
	D	sd	min	max	D	sd	min	max	
0	62.55	6.94	50.0	84.0	113.36	10.13	90.0	129.0	129,045
1	58.60	5.13	50.0	80.0	84.92	3.74	67.0	89.0	5,168
2	73.11	12.49	50.0	182.0	147.98	15.29	93.0	199.0	127,346
Total for classes	67.62	11.37	50.0	182.0	129.65	22.33	67.0	199.0	261,559

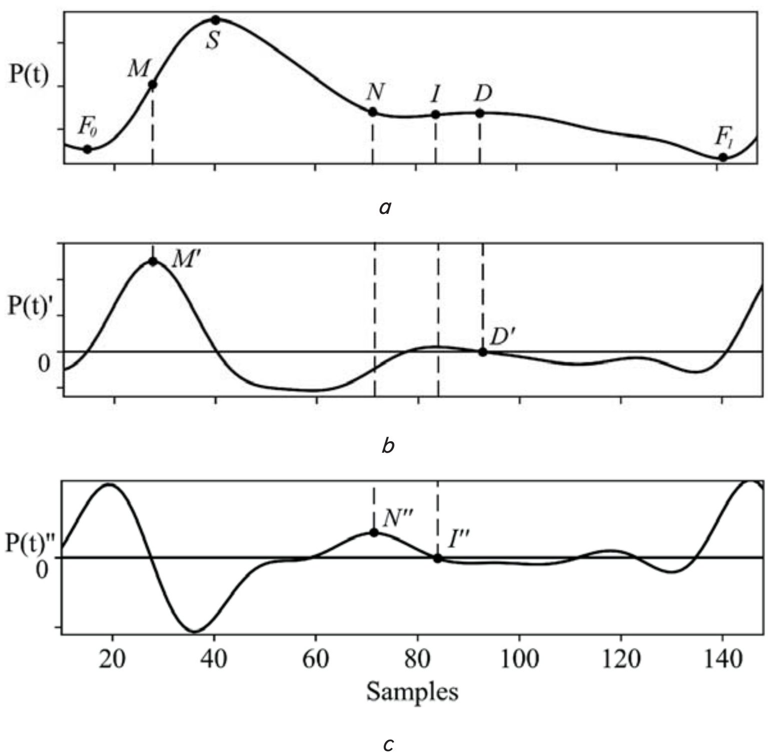

Fig. 4. Determining the position of the characteristic points of the pulse of the photoplethysmogram: *a* – signal of the photoplethysmogram $P(t)$; *b* – the first derivative of the $P(t)$ signal; *c* – the second derivative of the $P(t)$ signal

The position of the F_i points is determined by applying the AMPD algorithm to the inverted version of the PPG signal – $P(t)$.

In the second stage of the search for characteristic points, the position of the point of maximum inclination is determined (*M* in Fig. 4, *a*). It is always located on the ascending momentum between points F_0 and *S* and is determined by the maximum value of the first derivative of the signal $P(t)$', that is, point *M'* in Fig. 4, *b*.

The third step implies more complex procedures for determining the diastolic peak (point *D* in Fig. 4, *a*) since it can be weakly manifested in various forms of the PPG pulse (for example, as in the PPG signal in Fig. 2, *b*). In this regard, for the downward section of the momentum between points *S* and F_1, the procedure of spline interpolation with polynomials of the 7th power is applied to eliminate possible artifacts of the waveform [16]. For all subsequent actions, the first and second derivatives are calculated for the resulting approximated function $\hat{P}(t)$. Now, the position of the diastolic peak is taken as the point *D'*, where the first derivative is zero, and the second has a negative value.

In the fourth step, the location of the dicrotic notch at point *N* in Fig. 4, *a* is determined. Its position is at the local maximum of the second derivative of the function $\hat{P}(t)$ at the corresponding point *N''*, lying up to point *D* of the diastolic peak.

The fifth step determines the position of the inflection point *I*, which is between the dicrotic notch *N* and the diastolic peak *D*. In this segment, its position is taken as the position of point *I''*, where the second derivative of the function $\hat{P}(t)$ is zero. If it is not possible to determine the point *I''*, then point *I* is taken to lie in the middle of the segment *ND*.

After establishing the position of the characteristic points, the parameters of the PPG pulses are determined.

All digital signal processing and training sampling operations were performed in python 3.10 using the libraries numpy 1.22, scipy 1.7.3, pandas 1.3.5, pywavelets 1.2, neurokit2 0.1.5, pyampd 0.0.1.

Model training was performed using the scikit-learn 1.0.2 and xgboost 1.5.1 libraries.

5. Results of the study to devise a method for predicting blood pressure levels

5. 1. Defining informative features in the studied signals and the formation of a training data set

Fig. 5 shows the PPG pulse parameters used to construct informative features.

Table 3 describes the PPG pulse parameters used in accordance with Fig. 5.

It should be noted that when choosing informative features, parameters in the form of amplitude relations or areas of the pulse form of the PPG were purposefully used. This makes it possible to apply models trained on these features with various devices for taking PPG without the need to agree on measuring scales. In addition, at the stage of selecting features, the informativeness of the selected parameters of the PPG was taken into consideration when training classifier and regressor models. In addition to the pulse parameters of the PPG described in the literature, additional features were constructed, as shown in Table 3.

Thus, the feature space of each object in the training sample will represent the vector $x=(x^1, \ldots, x^d)$, where d=25 by the number of features used, including *ptt_p*, *ptt_m*, *ptt_f*, *hr*, as well as attributes from Table 3.

In the process of forming a training sample $X=(x_i, y_i)$ $^l{}_i$=1, the calculation of these features for the analyzed signals within a ten-second interval for each ECG complex and the PPG pulse was performed.

Due to artifacts of different nature, the shape of the signals can be severely distorted. Therefore, from the calculated series of values of the current parameter, those values that lie outside the range [Q_1–1.5·*IQR*: Q_3+1,5·*IQR*]. Here, Q_1, Q_3 are the first and third quartiles of the analyzed parameter, and *IQR* is its interquartile scope. For the remaining series of values, the arithmetic mean is determined, which is taken as the value of the current informative feature of this sample.

The parameter values calculated in this way *ptt_p, ptt_m, ptt_f* have strong outliers, up to 5–6 seconds, as shown by the box plots in Fig. 6, *a*.

It is obvious that such values are greatly inflated and indicate the incorrectness of some part of the analyzed data. Therefore, for the correct implementation of ML algorithms, the training sample was adjusted by filtering the outliers in the PTT parameters by 0.99 quantile, as shown in Fig. 6, *b*.

To train and test the models of the classifier and regressors, the resulting training sample *X* with a size of l=253624 was used. To select the ML a(x) algorithms, all data were randomly divided into two subsamples in the proportion of 9 to 1. Training and quality control of algorithms using cross-validation was performed on the first sub-sample, and the adequacy of the algorithms was checked on the second – control subsample

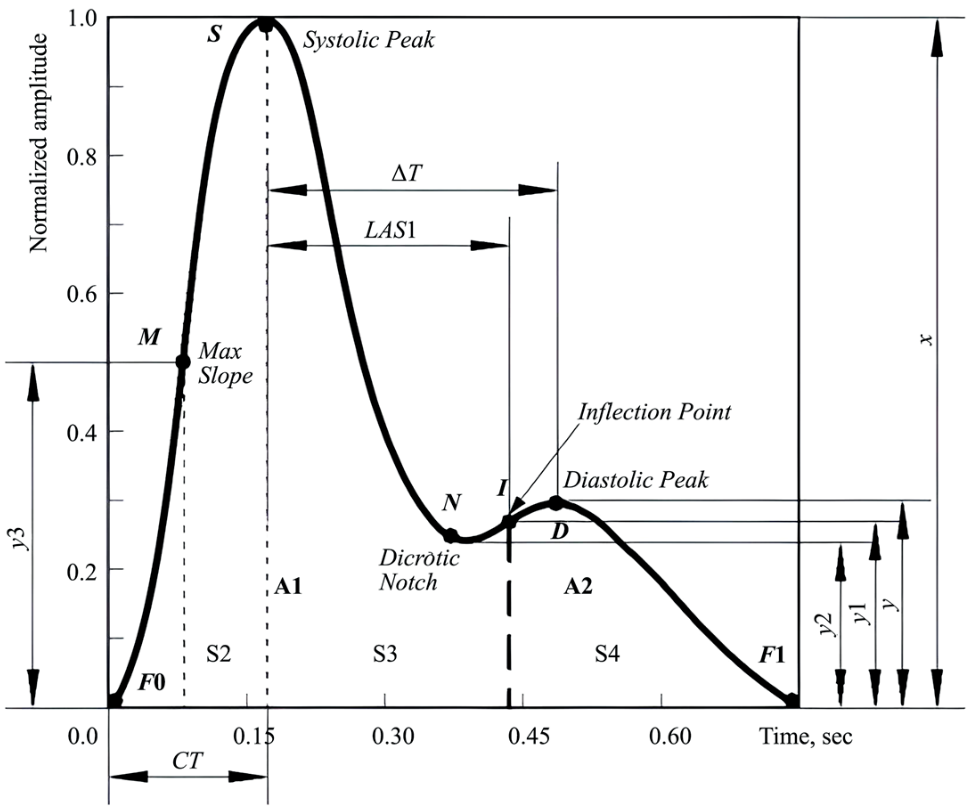

Fig. 5. Pulse parameters of the photoplethysmogram

Table 3

PPG impulse parameters

No.	Designation	Description
PPG pulse parameters described in the literature [21]		
1	ΔT	Time between systolic and diastolic peaks
2	*LASI*	Large Artery Stiffness Index represents the time interval between the systolic peak and the point of inflection
3	*CT*	Crest Time – time interval from the beginning of the impulse to the systolic peak
4	*AI*	Augmentation Index is defined as the ratio of the amplitude of the diastolic peak y to the amplitude of the systolic peak x: $AI=y/x$
5	*RI*	Reflection Index – this is the ratio of the pulse amplitude at the inflection point $y1$ to the amplitude of the systolic peak x: $RI=y1/x$
6	*IPA*	Inflection Point Area Ratio is calculated as the ratio of the area $A2$ under the impulse curve after the inflection point to the area $A1$ up to that point: $IPA=A2/A1$
7	$S/S2$, $S/S3$, $S/S4$	The ratio of the total area under the waveform curve S to the areas for different sections of the waveform between given characteristic points $S2$, $S3$, $S4$ [23]
Additional parameters of the PPG pulse		
8	T_{SF1}	Time interval between systolic peak and end of pulse
9	T_{SN}	Time interval between systolic peak and dicrotic notch
10	*NI*	The ratio of the pulse amplitude at the point of the dicrotic notch $y2$ to the amplitude of the systolic peak x: $NI=y2/x$
11	*MI*	The ratio of the pulse amplitude at the point of maximum slope $y3$ to the amplitude of the systolic peak x: $MI=y3/x$
12	T_{F0M}	Time interval between the start of the impulse and the point of maximum slope
13	T_{DF1}	Time interval between diastolic peak and end of impulse
14	tgα	The ratio of the amplitude of the systolic peak x to the value of the rise time CT: $\mathrm{tg}\alpha=x/CT$
15	tgβ	The ratio of the amplitude of the systolic peak x to the value T_{SF1}: $\mathrm{tg}\beta=x/T_{SF1}$
16	tgα’	The ratio of the pulse amplitude at the point of maximum slope $y3$ to the value T_{F0M}: $\mathrm{tg}\alpha'=y3/T_{F0M}$
17	tgβ’	The ratio of the amplitude of the diastolic peak y to the value T_{DF1}: $\mathrm{tg}\beta'=y/T_{DF1}$
18	T_{MN}	Time interval between the point of maximum slope and the dicrotic notch
19	T_{MD}	Time interval between the point of maximum inclination and the diastolic peak

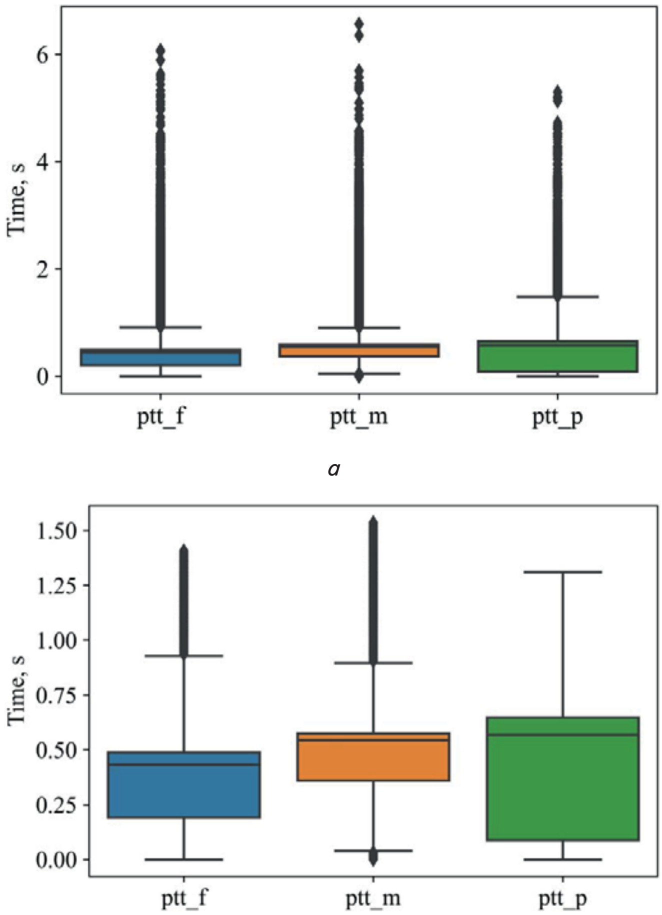

Fig. 6. Box plots for Pulse Transit Time features: *a* – calculated Pulse Transit Time parameters; *b* – adjusted Pulse Transit Time parameters

5. 2. Finding the optimal classifier model

The highest results in the classification task were achieved for random forest (Random Forest Classifier, RFC), *k*-nearest neighbors (k-Nearest Neighbors Classifier, kNNC) [24], and Extremely Randomized Trees Ensemble Classifier (ERTC) [25]. For these algorithms, optimal hyperparameters were selected. The model based on the *k* algorithm of the nearest neighbors was trained on the data with a standardized assessment made.

Table 4 gives the stratified five-fold cross-validation quality metrics of the classification of selected models.

The designations of quality metrics and hyperparameters, given in Table 4, correspond to those adopted in the python library scikit-learn [26]. The hyperparameter values, not listed in Table 4, are accepted as the default values.

As follows from Table 4, the model based on ERTC is slightly superior to RFC. The kNNC algorithm loses in the quality of the classification to ERTC and RFC. It is also obvious that due to the strong imbalance of classes (Table 2), the mean value of the *f*1-*score* (*macro*) metric differs significantly from its weighted value.

5. 3. Defining a training strategy for the classifier model

Fig. 7, *a* shows the quality metrics of the ERTC model for the available unbalanced dataset from a 25 % deferred subsample. Due to the much smaller number of Y=1 (low pressure) class samples, there are strong differences in *the precision* and *recall* metrics. To correct the imbalance, it is proposed to equalize the number of samples in the training subsample by adding synthetic data using the SMOTE method (Synthetic Minority Oversampling Technique) [27].

Fig. 7, *b* shows the quality metrics of the ERTC model on a deferred subsample for class-balanced data.

Table 5 gives the obtained quality metrics of the classification of this model. Fig. 8 shows the corresponding error matrix.

Table 5

ERTC model classification quality metrics

Feature classes and multiclass metrics	precision	recall	specificity	f1-score	Number of samples
Normal pressure	0.8717	0.8248	0.8798	0.8476	31,538
Low pressure	0.6826	0.6659	0.9935	0.6742	1,305
High pressure	0.8353	0.8825	0.8380	0.8582	30,563
Accuracy	–	–	–	0.8494	63,406
Macro mean	0.7965	0.7911	0.9038	0.7933	63,406
Weighted mean	0.8502	0.8492	0.8835	0.8492	63,406

Table 6 gives a comparison of the obtained classification results from this study with other works in the subject area under consideration.

Table 6 gives the research data of the multiclass classification metrics, the number of samples in the training sample, as well as the types of classes detected.

Table 4

Classifier models

Classifier $a(x)$	Hyperparameters	Quality metrics				
		Macro precision	Macro recall	Macro f1-score	Weighted f1-score	Micro f1-score
RFC	– number of trees *n_estimators*=463	0.8715	0.7146	0.7637	0.8435	0.8449
kNNC	– Minkowski metric p=1; – number of neighbors *n_neighbors*=6; – weight function *weights*=*'distance'*	0.8096	0.7323	0.7635	0.8243	0.8249
ERTC	– number of trees *n_estimators*=443	0.8733	0.7272	0.7746	0.8488	0.8504

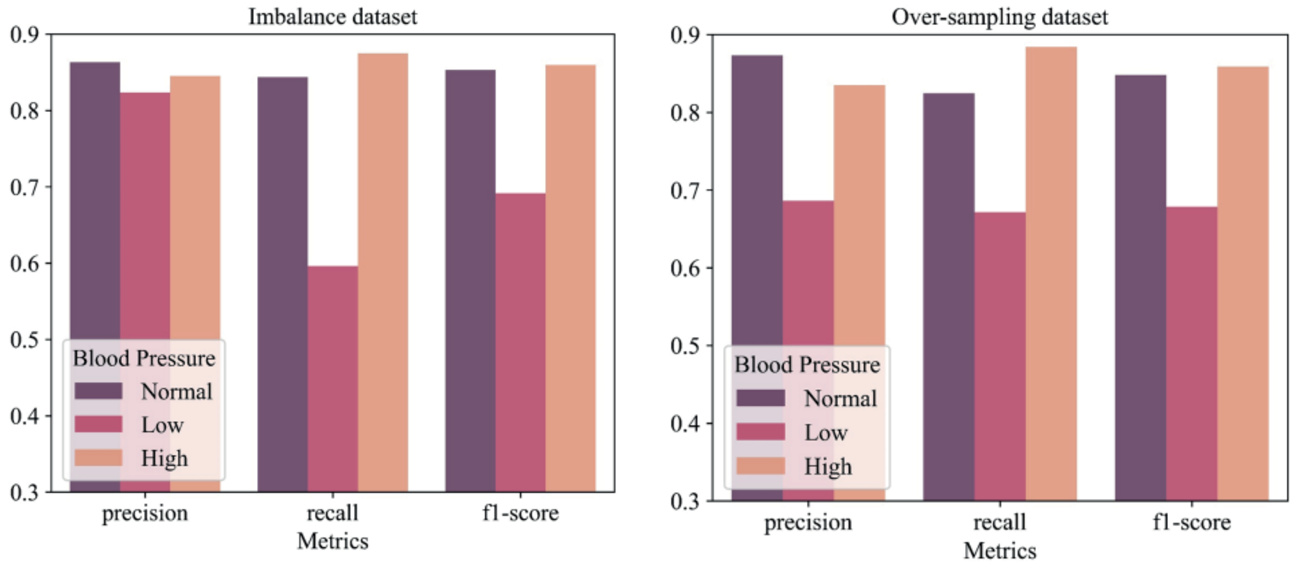

a *b*

Fig. 7. Comparison of classification quality indicators:
a – for an unbalanced data set; *b* – for balanced according to the SMOTE method

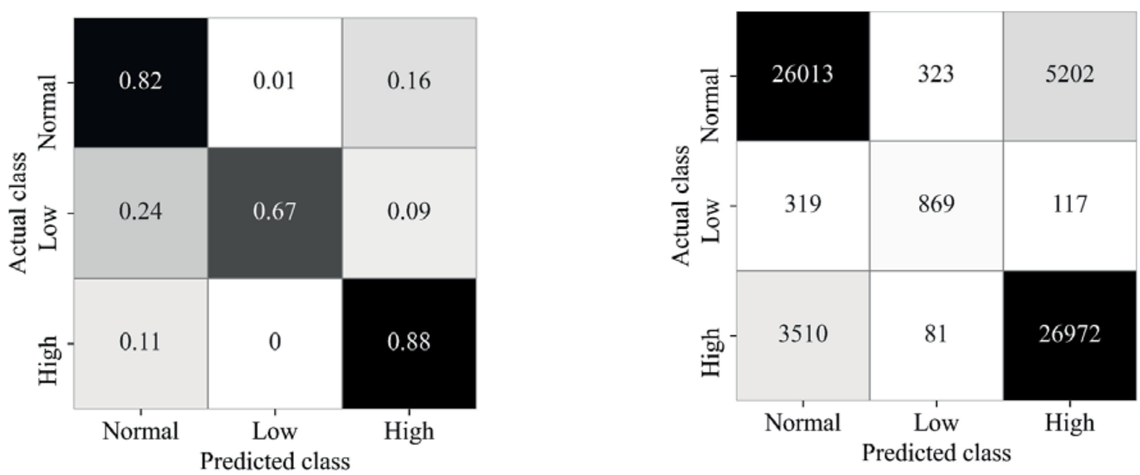

a *b*

Fig. 8. Error matrix of the Extremely Randomized Trees Ensemble Classifier:
a – by the number of samples; *b* – in percentage terms

Table 6

Comparison of the classification quality of the ERTC model with other studies

Metric	precision	recall	specificity	f1-score	Number of samples	Class	Reported in
Macro avg	No data	0.6930	0.8770	0.6840	942	Optimal/Normal/ High Normal/Grade 1 Hypertension/Grade 2 Hypertension/Grade 3 Hypertension/ Isolated Systolic Hypertension	[16]
Macro avg	No data	0.9426	0.9617	0.9484	80	Normal/Hypertension	[14]
Macro avg	No data	0.8392	0.8476	0.8434	87	Normal/Prehypertension	[14]
Macro avg	No data	0.8747	0.9593	0.8849	121	Normal +Prehypertension/ Hypertension	[14]
Macro avg	0,7965	0.7911	0.9038	0.7933	63406	Low/Normal/High	This work
Weighted avg	0,8502	0.8492	0.8835	0.8492	–		

5. 4. Construction of regression models and a general method for performing predictions

To build regression models according to the criterion of maximizing the coefficient of determination $R2$ and the minimum of the mean absolute error MAE, the algorithms $a(x)$, given in Table 7, were selected; it also lists the hyperparameters selected for them.

Table 7

Regression models

Regression model $a(x)$	Hyperparameters
Random forest (RFR)	– number of trees *n_estimators*=464
k-nearest neighbors (kNNR)	– Minkowski metric p=1; – Number of neighbors *n_neighbors*=6; – weight function *weights='distance'*
Gradient boosting (XGBR) [28]	– column subsampling relation when building each tree *colsample_bytree*=0.7; – learning rate *learning_rate*=0.1; – tree maximal depth *max_depth*=15; – the minimum sum of instance weights to split a node *min_child_weight*=6; – subsampling ratio of training instances *subsample*=0.95; – number of trees *n_estimators*=500
Extra Random Trees (ERTR)	– number of trees *n_estimators*=329

Fig. 9 shows the quality indicators of regression models for algorithms from Table 7 obtained by means of a five-fold cross-check.

According to the results obtained (Fig. 9), the most efficient algorithm is ERTR (SP: $R2$=0.6738±0.0017, MAE=8.6764±0.0291 mmHg; DP: $R2$=0.61031±0.005, MAE=4.4787±0.0033 mmHg; MeanP: $R2$=0.6627±±0.0035, MAE=5.0815±0.0154 mmHg).

However, to improve the regression characteristics, it is proposed to use a stacked generalization of algorithms [29] as an ensemble tool. To form meta-features, we used the best-found regression algorithm ERTR (*n_estimators*=100), as well as basic models of different nature: kNNR (p=1, *n_neighbors*=6, *weights='distance'*), ridge regression and Lasso regression with default parameters [26].

The role of a metamodel that performs the final forecast belongs to XGBR (*n_estimators*=50).

Fig. 10–12 show scatterplots with regression lines for the resulting metamodels on a deferred 25 % subsample. Fig. 10–12 also demonstrate the calculated median absolute *MedAE error.*

Fig. 13–15 also show the distributions of metamodel prediction errors for SP, DP, and MeanP, respectively.

To conduct a comparative assessment of the quality of forecasting the proposed regression metamodels, the protocol of the British Hypertension Society (BHS) can be used [30]. This protocol is used to assess the accuracy of BP measurement by various devices and methods and is widely used in practice. The BHS protocol is based on the calculation of percentiles for absolute error at its values of 5, 10, and 15 mmHg. At the same time, according to the results of measurements, three classes of accuracy of devices (methods) are determined – A, B, and C. Fig. 8 shows the requirements of BHS and the corresponding forecasting results achieved in the present study.

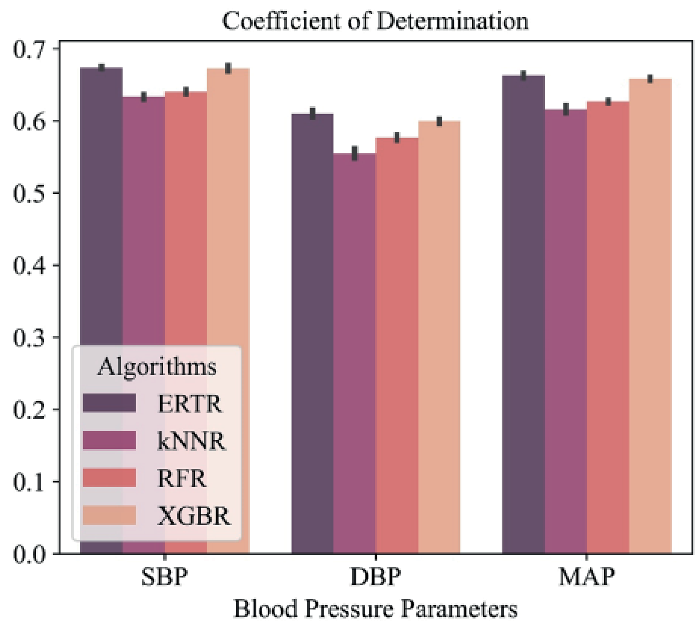

a

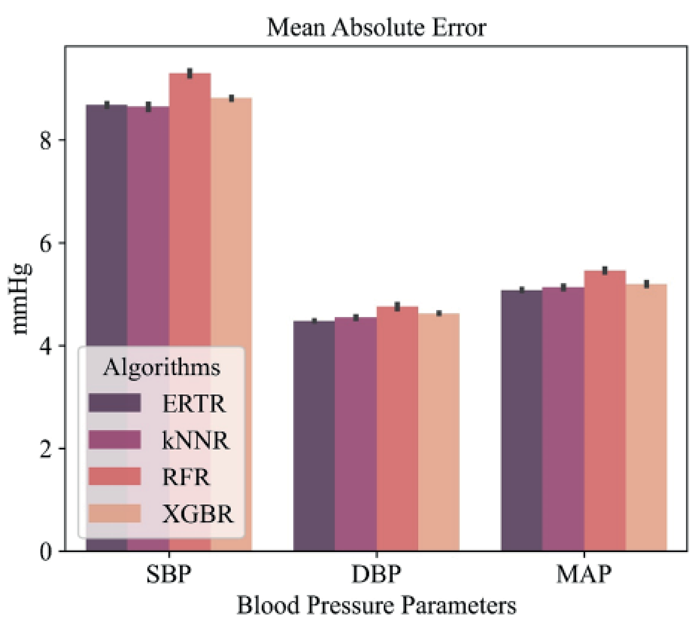

b

Fig. 9. Indicators of the quality of regression models: *a* – coefficient of determination; *b* – the mean absolute error

Table 8

Obtained forecasting results in comparison with the requirements of BHS

Absolute error		≤5 mmHg	≤10 mmHg	≤15 mmHg
This work	SP	52.26 %	72.71 %	83.33 %
	DP	71.8 %	89.44 %	95.80 %
	MeanP	67.88 %	86.61 %	94.32 %
BHS	class A	60 %	85 %	95 %
	class B	50 %	75 %	90 %
	class C	40 %	65 %	85 %

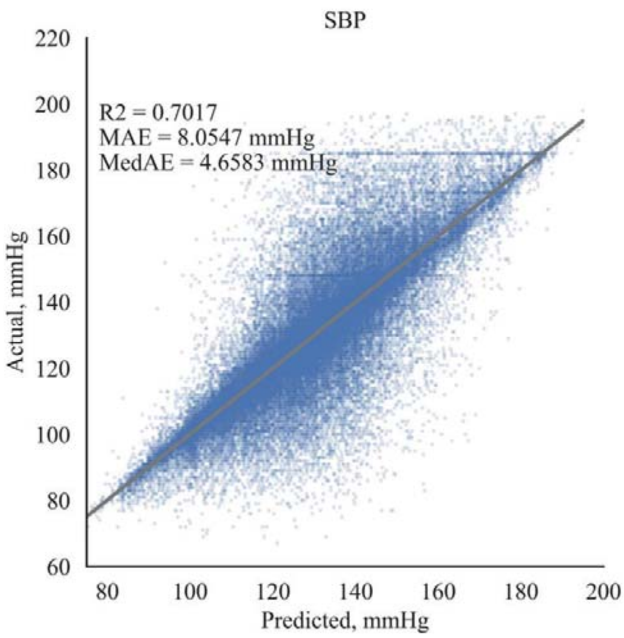

Fig. 10. Systolic pressure scatterplot

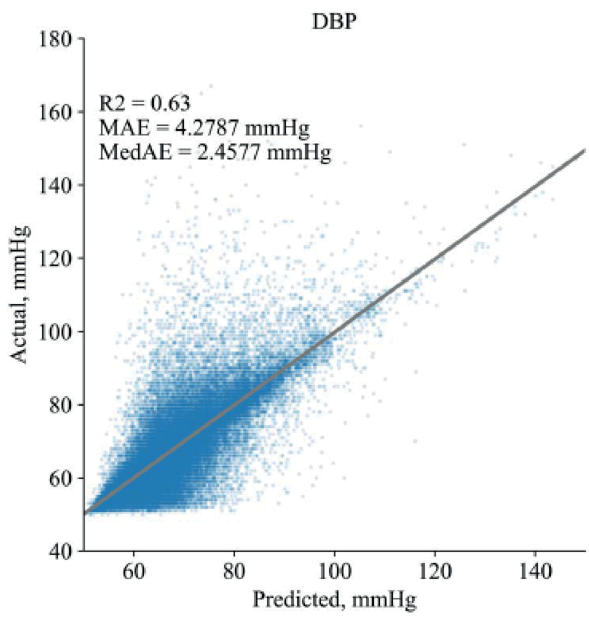

Fig. 11. Diastolic pressure scatterplot

In addition, the ANSI/AAMI SP10 (Association for the Advancement of Medical Instrumentation) standard can be used to assess the accuracy of BP forecasting [31]. Table 9 also provides comparative information on the requirements of ANSI/AAMI SP10 regarding the results of this study.

Table 9

ANSI/AAMI SP10 error limits compared to the results of this study

Parameter		*D*, mmHg	*sd*, mmHg	*n*
This work	SP	–0.0358	12.1843	≥85
	DP	–0.032	6.9092	≥85
	MeanP	–0.0352	7.3176	≥85
ANSI/AAMI SP10		0–0.5±	6.95–6.93	≥85

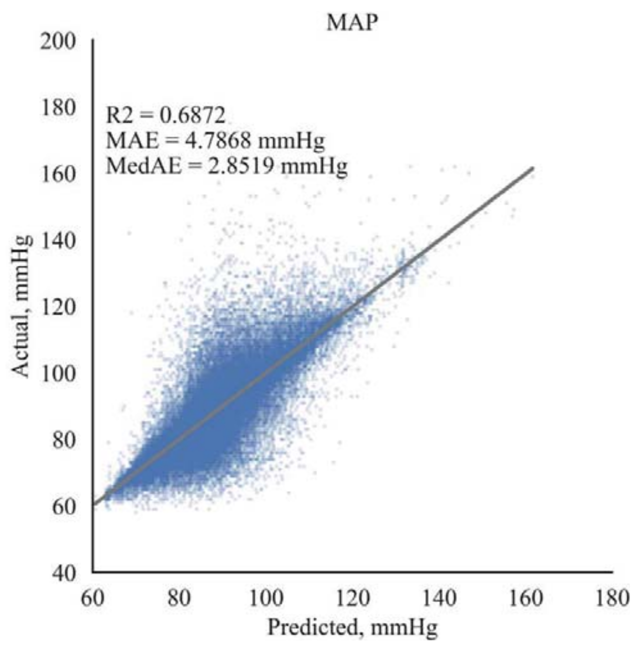

Fig. 12. Mean pressure scatterplot

This standard regulates the values of the sample mean *D* and the standard deviation *sd* for the measurement error calculated from a sample with the number of objects $n \geq 85$.

Based on the described solutions to the tasks set, a method for forecasting SP, DP, and MeanP, and/or classification of BP has been developed, the general structure of which is shown in Fig. 16.

As can be seen from the diagram in Fig. 16, at the initial stage, the ECG and PPG signals are filtered. Moreover, in addition to high-frequency filtering, in practice, it is also necessary to perform low-frequency filtering to eliminate interference and artifacts that occur during the recording process.

When designing low-pass digital filters, one should place the cut-off frequency below the AC frequency and avoid phase distortion.

On the filtered ECG signal (ECG filt. in Fig. 16), the positions of R-wave are determined. For the PPG filt signal, the position of the characteristic points is determined (Fig. 4). After that, 25 described informative features are calculated. Next, the calculated features are cleaned up – outliers in the data are not taken into consideration.

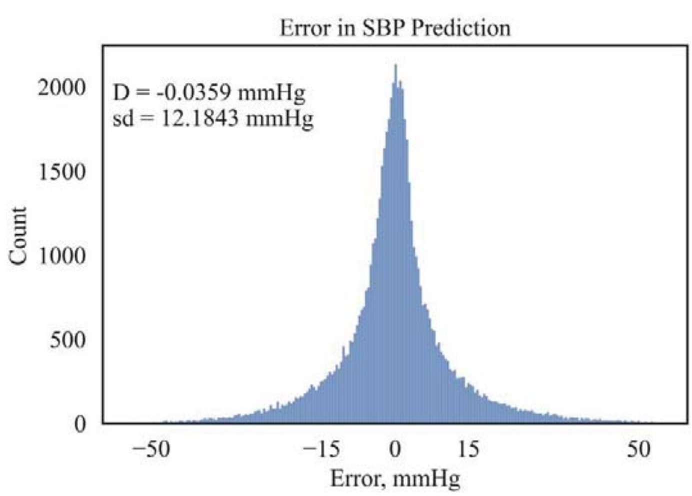

Fig. 13. Error distribution for systolic pressure predictions

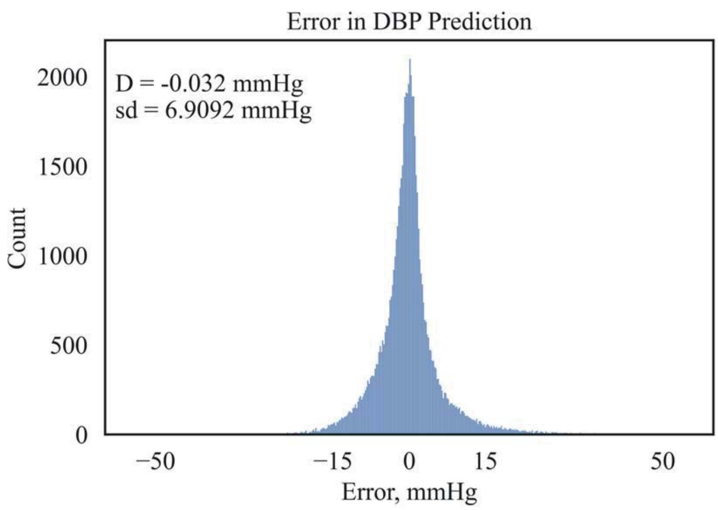

Fig. 14. Error distribution for diastolic pressure predictions

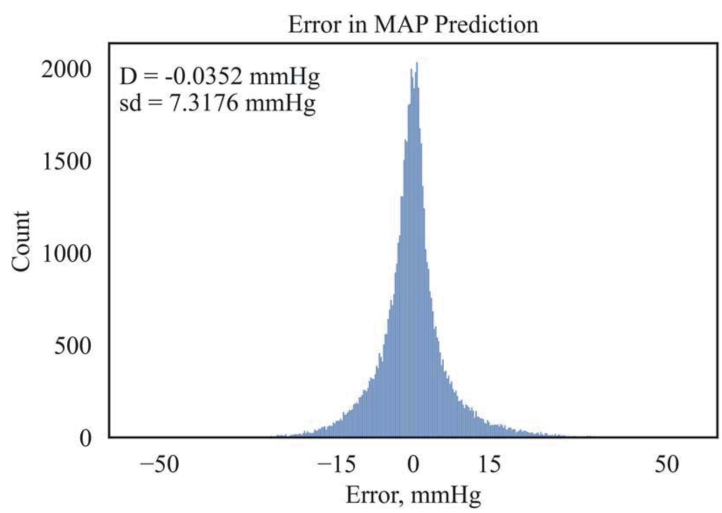

Fig. 15. Error distribution for mean pressure predictions

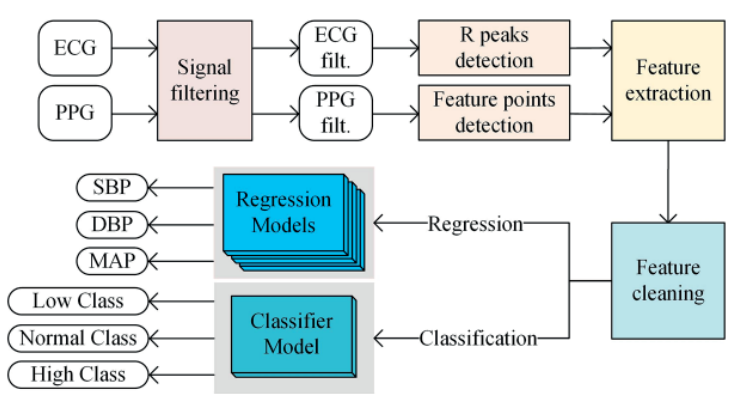

Fig. 16. Structure of the method of forecasting blood pressure and/or its classification

After that, according to Fig. 16, depending on the task being solved, the prediction of the parameters of SP, DP, and MeanP can be performed using the developed regression models, or the classification of BP into three classes based on the obtained classifier model can be conducted.

6. Discussion of results of the study to devise a method for predicting blood pressure levels

In the course of our study, the most optimal quality of classification was obtained on the ERTC model, built using a balanced training subsample.

As follows from Table 5 and Fig. 8, the developed classifier is more successful in the task of detecting high pressure (Y=2). This fact is especially important in the context of the problem being solved. The quality of the low-pressure classification (Y=1) is significantly lower, due to the insufficient number of samples in the data set used. However, when conducting screening studies, the task of identifying a low (reduced) BP will be less in demand. The training strategy using synthetic data makes it possible to eliminate the imbalance on *precision* and *recall*, as follows from Fig. 8. That, in turn, makes it possible to optimize the work of the classifier by the threshold of decision-making.

In accordance with Table 7, the quality of classification in work [14] exceeds the results of the present study. However, in [14], the number of samples is limited to the 121st record, which can significantly reduce the generalization ability of the model. In study [16], the authors implement a multiclass classification for 7 levels of BP from a sample of 942 samples. However, for screening studies, this approach may be redundant.

The results of the comparison, given in Tables 8, 9, show that the developed regression metamodels meet the requirements of the BHS class C protocol for forecasting SP; Class A for DP; class B for MeanP (absolute error differs from the requirements by 0.68 % only for values ≤15 mmHg). The requirements of ANSI/AAMI SP10 are met by the forecasts of the metamodel for DP. It can be assumed that the worst results of forecasting SP are associated with a higher variance of this parameter in the training sample (Table 2).

A distinctive feature of the proposed method is the use for forecasts of only signs of the FGG signal relative in the amplitude or area, which will allow the use of developed models with different types of sensors in terms of characteristics. In addition, time, frequency, or any other analysis of the ECG shape was not used to form the forecast. This makes it possible to reduce the number of informative features, as well as reduce the analysis time to 10-second intervals. It also makes it possible to use the ECG signal in any lead, for example, in the first standard lead (left and right hand), which is convenient to use for building mobile recorders.

The achieved quality of classification makes it possible to use the proposed model of the classifier to design devices for screening assessment of the level of BP or collect preliminary data. The proposed regression models, in terms of the quality of prediction, meet the requirements of BHS and, in part, the requirements of ANSI/AAMI SP10, and, therefore, can be used to monitor BP in the equipment of the corresponding accuracy class.

The limitations of the proposed method include the impossibility of its use to measure BP in children. Note the parameters of BP in childhood are different from adults.

To improve the quality of the presented method, it is necessary to increase the database for training classifier and regressor models. The more variable the data used in the training sample, the higher the generalizability of the developed models demonstrated.

At the time of writing this manuscript, we were testing a prototype of an electronic device that we designed, based on the MAX86150 biosensor (Maxim Integrated, USA). This device enables the prediction of the level of BP using the method described in this work.

7. Conclusions

1. In the process of our study, well-known informative features were isolated from the PPG signal according to the criterion of maximum information gain; we also defined the new ones. The resulting set of features together with the parameters PTT and heart rate made it possible to form a representative dataset ($X=\left(x_i,y_i\right)_{i=1}^{l=253624}$, $x=(x^1, ..., x^d)$, where d=25) for training ML models.

2. The analysis and testing of known ML algorithms have made it possible to identify the optimal model of the classifier based on the Extremely Randomized Trees ensemble Classifier algorithm, which showed the following quality metrics at cross-validation: *macro precision*=0.8733; *macro recall*=0,7272; *macro f1-score*=0,7746; *weighted f1-score*=0,8488; *micro f1-score*=0,8504.

3. When choosing a training strategy for the classifier, a strong imbalance of classes in the training set was accounted for. Given this, synthetic data generated by the SMOTE method were used to train the model. This has made it possible to optimize the value of the decision threshold with such parameters as *precision*=0.6826, *recall*=0.6659 for class Y=1.

4. We have built regression models to predict the value of SP, DP, and MeanP. For SP – $R2$=0,7071, MAE=8,0547 *mm*Hg, $MedAE$=4,6583 *mm*Hg, D=–0,0359 *mm*Hg, sd=12,1843 *mm*Hg. For DP – $R2$=0,63, MAE=4,2787 *mm*Hg, $MedAE$==2,4577 *mm*Hg, D=–0,032 *mm*Hg, sd=6,9092 *mm*Hg. For MeanP – $R2$=0,6872, MAE=4,7868 *mm*Hg, $MedAE$=2,8519 *mm*Hg, D=–0,0352 *mm*Hg, sd=7,3176 *mm*Hg. These indicators meet the requirements of BHS and make it possible to apply the proposed method of forecasting BP to design measuring equipment.

Conflict of interest

The authors declare that they have no conflict of interest in relation to this research, whether financial, personal, authorship or otherwise, that could affect the research and its results presented in this paper.

Acknowledgments

The authors express their gratitude to the Ministry of Science and Higher Education of the Republic of Kazakhstan for financial support (NTP No. O.0971) and the Institute of Mechanics and Mechanical Engineering named after Academician U. Dzholdasbekov.

References

1. Zhou, B., Carrillo-Larco, R. M., Danaei, G., Riley, L. M., Paciorek, C. J., Stevens, G. A. et. al. (2021). Worldwide trends in hypertension prevalence and progress in treatment and control from 1990 to 2019: a pooled analysis of 1201 population-representative studies with 104 million participants. The Lancet, 398 (10304), 957–980. doi: https://doi.org/10.1016/s0140-6736(21)01330-1
2. Hypertension (2021). World Health Organization (WHO). Available at: https://www.who.int/en/news-room/fact-sheets/detail/hypertension
3. Williams, B., Mancia, G., Spiering, W., Agabiti Rosei, E., Azizi, M., Burnier, M. et. al. (2018). 2018 ESC/ESH Guidelines for the management of arterial hypertension. European Heart Journal, 39 (33), 3021–3104. doi: https://doi.org/10.1093/eurheartj/ehy339
4. Peter, L., Noury, N., Cerny, M. (2014). A review of methods for non-invasive and continuous blood pressure monitoring: Pulse transit time method is promising? IRBM, 35 (5), 271–282. doi: https://doi.org/10.1016/j.irbm.2014.07.002
5. Pandit, J. A., Lores, E., Batlle, D. (2020). Cuffless Blood Pressure Monitoring. Clinical Journal of the American Society of Nephrology, 15 (10), 1531–1538. doi: https://doi.org/10.2215/cjn.03680320
6. Mukkamala, R., Stergiou, G. S., Avolio, A. P. (2022). Cuffless Blood Pressure Measurement. Annual Review of Biomedical Engineering, 24 (1), 203–230. doi: https://doi.org/10.1146/annurev-bioeng-110220-014644
7. Figini, V., Galici, S., Russo, D., Centonze, I., Visintin, M., Pagana, G. (2022). Improving Cuff-Less Continuous Blood Pressure Estimation with Linear Regression Analysis. Electronics, 11 (9), 1442. doi: https://doi.org/10.3390/electronics11091442
8. Stergiou, G. S., Mukkamala, R., Avolio, A., Kyriakoulis, K. G., Mieke, S., Murray, A. et. al. (2022). Cuffless blood pressure measuring devices: review and statement by the European Society of Hypertension Working Group on Blood Pressure Monitoring and Cardiovascular Variability. Journal of Hypertension, 40 (8), 1449–1460. doi: https://doi.org/10.1097/hjh.0000000000003224
9. Nour, M., Polat, K. (2020). Automatic Classification of Hypertension Types Based on Personal Features by Machine Learning Algorithms. Mathematical Problems in Engineering, 2020, 1–13. doi: https://doi.org/10.1155/2020/2742781
10. Ibrahim, B., Nathan, V., Jafari, R. (2017). Exploration and validation of alternate sensing methods for wearable continuous pulse transit time measurement using optical and bioimpedance modalities. 2017 39th Annual International Conference of the IEEE Engineering in Medicine and Biology Society (EMBC). doi: https://doi.org/10.1109/embc.2017.8037256
11. Thambiraj, G., Gandhi, U., Mangalanathan, U., Jose, V. J. M., Anand, M. (2020). Investigation on the effect of Womersley number, ECG and PPG features for cuff less blood pressure estimation using machine learning. Biomedical Signal Processing and Control, 60, 101942. doi: https://doi.org/10.1016/j.bspc.2020.101942

12. Saeed, M., Villarroel, M., Reisner, A. T., Clifford, G., Lehman, L.-W., Moody, G. et. al. (2011). Multiparameter Intelligent Monitoring in Intensive Care II: A public-access intensive care unit database*. Critical Care Medicine, 39 (5), 952–960. doi: https://doi.org/10.1097/ccm.0b013e31820a92c6
13. Sanuki, H., Fukui, R., Inajima, T., Warisawa, S. (2017). Cuff-less Calibration-free Blood Pressure Estimation under Ambulatory Environment using Pulse Wave Velocity and Photoplethysmogram Signals. Proceedings of the 10th International Joint Conference on Biomedical Engineering Systems and Technologies. doi: https://doi.org/10.5220/0006112500420048
14. Liang, Y., Chen, Z., Ward, R., Elgendi, M. (2018). Hypertension Assessment via ECG and PPG Signals: An Evaluation Using MIMIC Database. Diagnostics, 8 (3), 65. doi: https://doi.org/10.3390/diagnostics8030065
15. Miao, F., Liu, Z.-D., Liu, J.-K., Wen, B., He, Q.-Y., Li, Y. (2020). Multi-Sensor Fusion Approach for Cuff-Less Blood Pressure Measurement. IEEE Journal of Biomedical and Health Informatics, 24 (1), 79–91. doi: https://doi.org/10.1109/jbhi.2019.2901724
16. Hasanzadeh, N., Ahmadi, M. M., Mohammadzade, H. (2020). Blood Pressure Estimation Using Photoplethysmogram Signal and Its Morphological Features. IEEE Sensors Journal, 20 (8), 4300–4310. doi: https://doi.org/10.1109/jsen.2019.2961411
17. Kachuee, M., Kiani, M. M., Mohammadzade, H., Shabany, M. (2015). Cuff-less high-accuracy calibration-free blood pressure estimation using pulse transit time. 2015 IEEE International Symposium on Circuits and Systems (ISCAS). doi: https://doi.org/10.1109/iscas.2015.7168806
18. DeMers, D., Wachs, D. (2022). Physiology, Mean Arterial Pressure. StatPearls. Available at: https://www.ncbi.nlm.nih.gov/books/NBK538226/
19. Meng, L., Yu, W., Wang, T., Zhang, L., Heerdt, P. M., Gelb, A. W. (2018). Blood Pressure Targets in Perioperative Care. Hypertension, 72 (4), 806–817. doi: https://doi.org/10.1161/hypertensionaha.118.11688
20. Guzman, J. C., Melin, P., Prado-Arechiga, G. (2017). Design of an Optimized Fuzzy Classifier for the Diagnosis of Blood Pressure with a New Computational Method for Expert Rule Optimization. Algorithms, 10 (3), 79. doi: https://doi.org/10.3390/a10030079
21. Elgendi, M. (2012). On the Analysis of Fingertip Photoplethysmogram Signals. Current Cardiology Reviews, 8 (1), 14–25. doi: https://doi.org/10.2174/157340312801215782
22. Scholkmann, F., Boss, J., Wolf, M. (2012). An Efficient Algorithm for Automatic Peak Detection in Noisy Periodic and Quasi-Periodic Signals. Algorithms, 5 (4), 588–603. doi: https://doi.org/10.3390/a5040588
23. Kachuee, M., Kiani, M. M., Mohammadzade, H., Shabany, M. (2017). Cuffless Blood Pressure Estimation Algorithms for Continuous Health-Care Monitoring. IEEE Transactions on Biomedical Engineering, 64 (4), 859–869. doi: https://doi.org/10.1109/tbme.2016.2580904
24. Hasan, O. S., Saleh, I. A. (2021). Development of heart attack prediction model based on ensemble learning. Eastern-European Journal of Enterprise Technologies, 4 (2 (112)), 26–34. doi: https://doi.org/10.15587/1729-4061.2021.238528
25. Geurts, P., Ernst, D., Wehenkel, L. (2006). Extremely randomized trees. Machine Learning, 63 (1), 3–42. doi: https://doi.org/10.1007/s10994-006-6226-1
26. Pedregosa, F. et. al. (2011). Scikit-learn: Machine Learning in Python. Journal of Machine Learning Research, 12, 2825–2830. Available at: https://www.jmlr.org/papers/volume12/pedregosa11a/pedregosa11a.pdf
27. Chawla, N. V., Bowyer, K. W., Hall, L. O., Kegelmeyer, W. P. (2002). SMOTE: Synthetic Minority Over-sampling Technique. Journal of Artificial Intelligence Research, 16, 321–357. doi: https://doi.org/10.1613/jair.953
28. Chen, T., Guestrin, C. (2016). XGBoost: A Scalable Tree Boosting System. Proceedings of the 22nd ACM SIGKDD International Conference on Knowledge Discovery and Data Mining. doi: https://doi.org/10.1145/2939672.2939785
29. Wolpert, D. H. (1992). Stacked generalization. Neural Networks, 5 (2), 241–259. doi: https://doi.org/10.1016/s0893-6080(05)80023-1
30. O'Brien, E., Petrie, J., Littler, W., de Swiet, M., Padfield, P. L., O'Malley, K. et. al. (1990). The British Hypertension Society protocol for the evaluation of automated and semi-automated blood pressure measuring devices with special reference to ambulatory systems. Journal of Hypertension, 8 (7), 607–619. doi: https://doi.org/10.1097/00004872-199007000-00004
31. ANSI/AAMI SP10:2002/(R)2008 & ANSI/AAMI SP10:2002/A1:2003/(R)2008 & ANSI/AAMI SP10:2002/A2:2006/(R)2008. Manual, electronic, or automated sphygmomanometers. Association for the Advancement of Medical Instrumentation.